steel research international
www.steel-research.de

Study on the Pneumatic Lime Injection in the Electric Arc Furnace Process: An Evaluation on the Performance Benefits

Davide Mombelli, Gianluca Dall'Osto, Giacomo Villa, Carlo Mapelli, Silvia Barella, Andrea Gruttadauria, Lorenzo Angelini, Christian Senes, Massimiliano Bersani, Piero Frittella, Roberto Moreschi, Roberto Marras, and Giorgio Bruletti*

The pneumatic lime injection during the electric arc furnace (EAF) process by insufflation lances mounted on the furnace walls has gained much interest in the latest years. The main advantages, in comparison to the traditional procedure of lime lumps addition within the scrap bucket, can be summarized in raw materials consumption reduction, foaming benefits, operational cost benefits, and improvement in environmental aspects. In the proposed work, the advantages of a new lime injection system developed by Unicalce S.p.A. and installed on a 90 t EAF of Acciaierie di Calvisano are analyzed. Data from more than 1200 heats are acquired and compared with the traditional practice from an energetically and emissions point of view. To evaluate the benefits on the slag foamability, several slag samples, taken at the beginning and at the end of refining stage, are analyzed through isothermal solubility diagrams (ISDs). The ISD analysis results are then compared and validated with the total harmonic distortion (THD) of the arc in the corresponding heat. The upgrade to lime injection drives to considerable savings in electrical consumptions, oxygen, methane, and lime, with an overall save of more than 4,000 t year^{-1} of equivalent CO_2.

1. Introduction

Over the years the production of steel through electric arc furnace (EAF) technology has increased more and more, allowing the EAF to compete more successfully with the integrated mills; to the will to reduce the amount of CO_2 and dust emission have further encouraged the steel production through this technology. In 2019, the EAF crude steel production reached 517 million tons, corresponding to the 27.7% of the worldwide production.[1] In Italy, the scrap-based route covers a crucial role with 37 EAF production sites and a crude steel production share of 82%.[2,3]

The electric furnace process has evolved becoming a highly efficient scrap smelter, which integrate a technology able to improve energy using oxygen, gas, carbon, and lime injection. Generally, the lime charging procedure into the EAF is based on lime addition, in the form of lumps, directly within the scrap bucket through conveyor systems. This practice, however, has several issues related with lime emissions during the scrap bucket charging and an inadequate distribution of lime in the furnace, made possible instead by lime injection.[4] In recent years, the usage of pneumatic injection of lime in EAFs, due to its surprising results in terms of reduction of the specific raw material consumption, foaming benefits, operational cost benefits, and improvement in environmental aspects, has acquired interest as a viable technology for the steelmaking industry.[5]

Acciaierie di Calvisano steelmaking plant, in collaboration with Unicalce S.p.A., decided to upgrade its EAF, implementing a new system of lime delivering, in place of the traditional procedure. Combining carbon and lime powder injectors, the lances are able to create a homogeneous layer of foamy slag over the whole metal bath surface. The addition of lime is essential for the proper bath chemistry and the slag foaming practice, which offers an increased energy efficiency of the furnace, since the heat from the arc is captured by the slag; a protection of the water panels and the roof from radiation and a decreased noise pollution and low nitrogen incorporation in the steel are

D. Mombelli, G. Dall'Osto, G. Villa, Prof. C. Mapelli, Prof. S. Barella, A. Gruttadauria
Politecnico di Milano
Dipartimento di Meccanica
Via La Masa 1, 20156 Milano, Italy
E-mail: davide.mombelli@polimi.it

L. Angelini, C. Senes, M. Bersani, P. Frittella
Feralpi Holding S.p.A
Via Carlo Nicola Pasini 11, 25017 Lonato del Garda (BS), Italy

Dr. R. Moreschi, R. Marras, G. Bruletti
Unicalce S.p.A
Via Ponti 18, 24012 Val Brembilla (BG), Italy

The ORCID identification number(s) for the author(s) of this article can be found under https://doi.org/10.1002/srin.202100083.

DOI: 10.1002/srin.202100083

achieved.[6–9] The lime presence is also essential for carrying out the dephosphorization during the refining of the bath. If not removed, phosphorus has detrimental effects on the mechanical properties of the steel. Therefore, highly available CaO in the slag allows to decrease the phosphorus content of the bath trough the generation of tricalcium phosphate compounds ($3CaO{\cdot}P_2O_5$) which are captured by the slag.[10] The thermodynamic of the process is ruled by the content of lime in the slag, the higher the content the better the dephosphorization, whereas the kinetic is controlled by the dissolution rate of lime into the slag, the finer the lime the fastest the dephosphorization.[10,11]

The aim of this work is to evaluate and validate the potential benefits of injecting lime in fine particles, compared to the standard technique. For this purpose, data from more than 1200 heats were acquired and, so as to estimate the slag foaming evolution, further 23 heat slag samples were taken both at the beginning and end of refining, for a total of 46 samples. Tests were conducted in a 90 t top-charge EAF equipped with a wall-mounted, multipoint injecting system (carbon, lime, oxygen, and burners) on two different steel grades: special steels and structural steels, representing most of the steel production of the partner plant. Four injection points are available, three in the cold spots and one over the eccentric bottom tap-hole (EBT) (**Figure 1**). However, carbon and lime are only introduced at #1 and EBT positions. The reason lies in the fact that the exhaust gases evacuation system is placed over the position #3 and this can suck the carbon and lime powders. In addition, position #2 has been abolished due to an excessive refractory wear in the surrounding areas.

Three different lime addition procedures were considered: STD (the traditional procedure), INJ1, and INJ2 (lime injection procedure with a different amount of injected lime).

Electrical, oxygen, methane, lime consumptions, carbon, and slag production were evaluated and correlated with the slag foamability through isothermal solubility diagram (ISD) and total harmonic distortion (THD) values. Then, for a better comprehension of benefits of lime injection, a microstructure characterization of the collected slag was conducted. Finally, the environmental impact was investigated analyzing the tons of oil equivalent (TOE) and CO_2 emission reduction, for electrical and CH_4 savings.

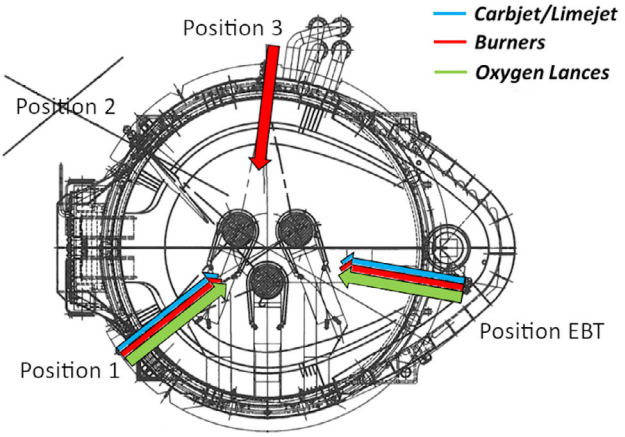

Figure 1. Schematic positions of multipoint injection system.

2. Experimental Section

2.1. Operational Profile

The furnace operational profiles had been divided in three procedures: STD, INJ1, and INJ2. STD profile indicated the traditional procedure used before the lime injection adoption. It consisted in using lime (20–30 wt.% MgO–80–70 wt.% CaO) in lumps directly loaded in each bucket. This procedure provided different amount of lime per bucket, depending on whether steel grades (special steels: three buckets or structural steels: four buckets). Approximately 4000 kg of lime lumps was used in STD procedure, equally divided on each bucket. INJ1 profile represented the pattern used insufflating lime and was adopted for both types of steel. This procedure required lime with different chemical composition and size: 1) injected lime (18 mesh): 15 wt.% MgO–75 wt.% CaO; 2) lime in lumps (30–50 mm; $t_{50} = 1.5$–2 min according to EN 459-2:2010): 20–30 wt.% MgO–80–70 wt.% CaO.

INJ2 procedure was a variant of INJ1, with an ≈400 kg more of injected lime.

As the injection system provided two lime injection points, each injection unit consisted of a pneumatic propeller with a capacity of 2200 L, equipped with a three-cell weighing system and a modulating extraction valve to regulate and control the lime injection flow rate on the active lance. The lime powder from the storage silo was loaded in a defined quantity by means of a weighing system into the pneumatic thruster through the servo-controlled spherical valve positioned on the head of the same, then it was transferred from here pneumatically and blown into the EAF. The flow rate of lime for each injection lance was in the range of 40–100 kg min^{-1}. The dry air consumption for each pneumatic drive was 400 $Nm^3 h^{-1}$. The injection system operated in the diluted phase, and the solids loading ratio (mass flow rate of conveyed material/mass flow rate of air) was between 4.6 and 11.6. The maximum amount of injected lime per heat was 1500 kg in 12–13 min.

Given the limited capacity of powder lime injection plant, roughly 1000 kg of lime in lumps was still charged in the first bucket for both the steels and both the IN1/INJ2 procedures. Then, from the second bucket, a specific amount of lime was injected at a specific melting percentage. Final lime injection was performed at the beginning of refining stage.

2.2. Data Collection

To validate the new operative practice, 1204 heats per type had been analyzed. They were divided as reported in **Table 1**. The analyzed data were as follows: CaO consumption; electric consumption; CH_4 consumption; O_2 consumption; carbon powder consumption; slag production; and characteristics.

Statistical analysis had been performed to compare the different procedures by means of the Tukey's method[12] throughout the software MINITAB.

Table 1. Experimental plan design.

Steel grade	Procedure	N° of heats
Special steel (three buckets)	STD	231
	INJ1	160
	INJ2	163
Structural steel (four buckets)	STD	429
	INJ1	150
	INJ2	71

2.3. Slag Sampling and Foamability Analysis

To evaluate the benefit of lime injection on the slag foamability, for 23 specific heats, the slag was sampled and analyzed for both types of steel: 10 heats for special steel and 13 heats for structural steel. Slag specimens were sampled due to an automated lance through the slag door then fast cooled by dripping it on the floor and sent to the laboratory where they were milled, pressed, and analyzed by means of X-ray fluorescence (XRF). For each heat, two samples were collected as follows: 1) a first sample at the beginning of refining stage (≈1580 °C); 2) a second sample at the ending of refining stage (≈1625 °C).

In such a way, the evolution of slag during the refining stage was followed for both the procedures: traditional (STD) and injection (INJ1/INJ2).

By measuring the slag average chemical composition through XRF analysis, the ISD based on BI_3 basicity (Equation (1)) index was recalculated by applying the Pretorius's model,[13,14] correcting the dual saturation point with respect to the Al_2O_3 concentration and considering a temperature equal to 1600 °C. The obtained diagrams had been compared between STD and INJ procedures, to check if the optimum foaming condition was reached. To validate the analysis on foamability based on ISD diagrams, the THD of the corresponding heat was acquired.[15]

$$BI_3 = \frac{CaO(wt.\%)}{(SiO_2 + Al_2O_3)(wt.\%)} \quad (1)$$

Low values of THD can be used to assert if a good quality foaming slag was being produced inside the EAF. The scale of THD interpretation was the following: 1) THD 10: perfectly covered arc—good slag foaming—best condition; 2) THD 11: well-covered arc—acceptable condition; 3) THD 12: partially uncovered arc—not so acceptable condition, need for minor corrections; 4) THD 13: arc uncovered—unacceptable condition, need for major corrections.

Microstructural and local chemical compositions of the different slag were performed by scanning electron microscopy (SEM) analysis (Zeiss, EVO 50) coupled with energy-dispersive spectroscopy (EDS) probe (INCA Oxford) on a polished section of a cold-mounted slag sample.

3. Results and Discussion

3.1. Analysis of CaO Consumptions

Switching from lump lime procedure to injected lime system led to a considerable CaO reduction in term of lime usage (**Figure 2**). Analysis showed a difference between STD versus INJ1 and STD versus INJ2 of ≈1000 kg and ≈800 kg, respectively, for special steels (Figure 2a,b). The same results were found for structural steels. The only difference is related to the higher difference between standard procedure and lime injection, namely, ≈1150 kg less for INJ1 and ≈950 kg less for INJ2 compared to STD (Figure 2c,d). Although the significative reduction in the CaO amount of the slag, for all the heats analyzed, the P target was reached. This was due to the faster dissolution kinetics of the lime into the molten slag, assuring a faster dephosphorizing capacity. In other words, being the lime powder faster dissolved into the molten slag than the lime lumps, dephosphorization started at a lower temperature, therefore improving the P-sizing effect of the slag.[10,16]

3.2. Analysis of Electrical Consumptions

As can be noted from **Figure 3**a,b, electrical consumption for the production of special steel is significantly different from STD to INJ procedures. The difference, from STD to INJ1 and STD to INJ2, turn out to be ≈30 and 35 kWh t^{-1}, respectively. The same result was observed for structural steels, even the electrical consumption increased as increasing the injected lime amount in INJ2 procedure (the electrical saving decreased from 30 to 20 kWh t^{-1}) (Figure 3c,d). This can be related to the wide variation of scraps quality, that imply more oxidizable scraps (e.g., the ones with a high surface over volume ratio) and thus, higher amount of slag needs to be heated, requiring more electrical power.[17]

To better understand at which stage of the EAF process the electrical savings are concentrated, the energy distribution across melting and refining stages was determined. In **Figure 4**, the amount of energy consumed during the refining stage is reported. The trend of energy savings during refining is coherent with the overall electrical energy consumption reduction shown in Figure 3.

The mean values in Figure 4 show how most of the electrical saving is concentrated during the refining stage. Actually, compared to the total saving of 30 kWh t^{-1}, the consumption improvement during the refining accounts for ≈20 kWh t^{-1}. This implies that ≈66.5% of the saving is concentrated in the last stage of the process, whereas the remaining portion is split among the buckets melting stage. The reason should be related with the reduction of 1 t of lime, which means a lesser amount of material to be melted, together to a better foaming condition. In particular, this last assumption will be discussed more in detail in Section 3.6. For the special steels, the same trend is replicated (Figure 4c,d).

The introduction of lime injection has also allowed for a reduction in the power-on time of about 1.5 min with respect to the traditional procedure, as shown in **Figure 5**. This explains the additional energy savings registered and not depending by refining. Even for structural steels, being energy savings lower than those above as well, the saving is mostly concentrated in refining stage, whereas the remaining part is divided between

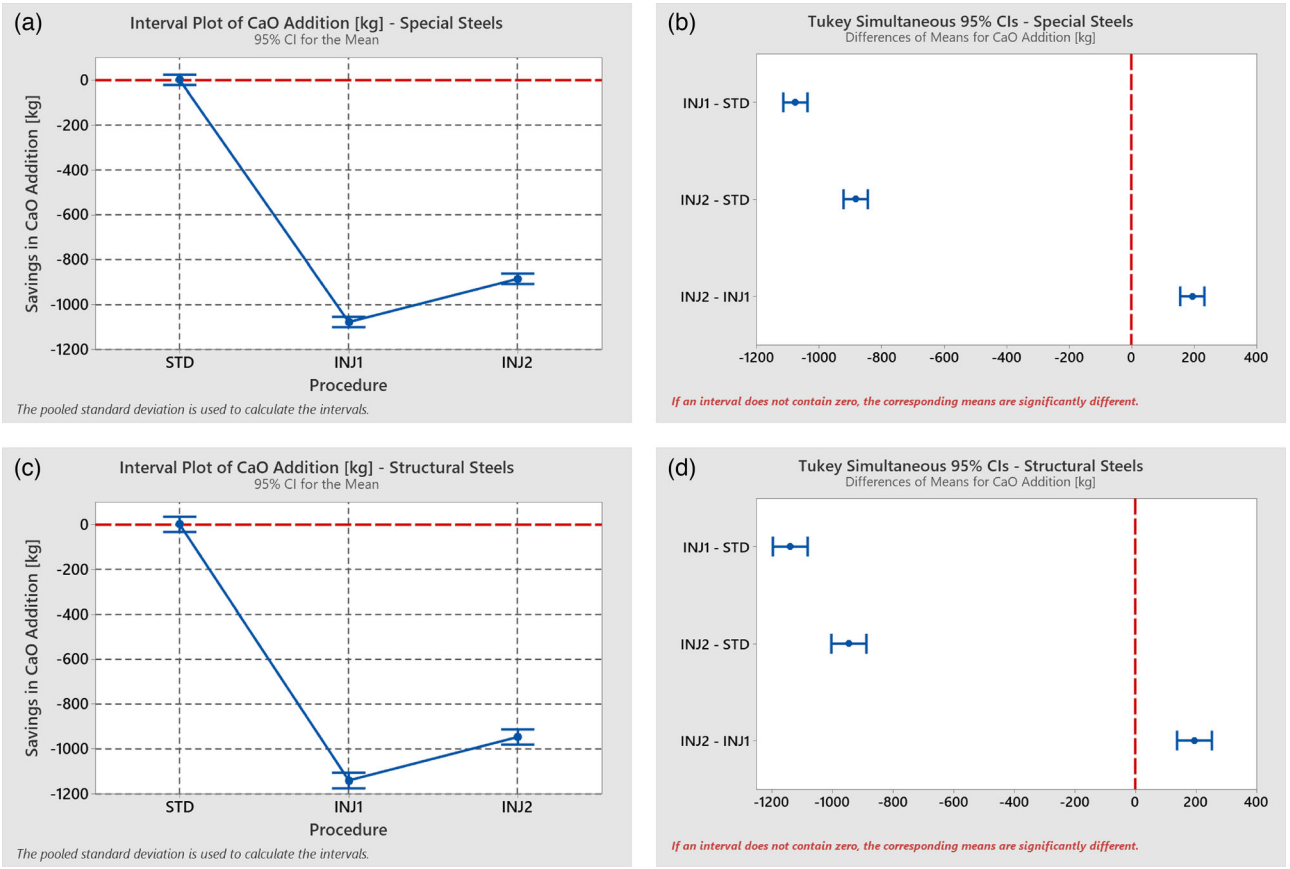

Figure 2. Variation of lime consumption switching from STD procedure to INJ1/2 procedures: a) interval plot, b) Tukey's comparison for special steels; c) interval plot, and d) Tukey's comparison for structural steels (values in kg).

the four buckets melting stage as a reduction of power-on times (Figure 5c,d). As anticipated before, even in this case the power-on decreases due to the lower amount of used lime (≈1 t less), as well as a better energy concentration in the bath during refining, due to a better foaming.

To evaluate the enhancing of the furnace performances, brought by the injection procedure, the experimental energy savings were compared with the theoretical ones evaluated through the Köhle method (Equation (2)).[17,18]

$$\frac{W_R}{\mathrm{kWh\ t^{-1}}} = 300 + 900 \cdot \left[\frac{G_E}{G_A} - 1\right] + 1600 \cdot \frac{G_Z}{G_A} + 0.7 \cdot \left[\frac{T_A}{^\circ C} - 1600\right] + 0.85 \cdot \frac{t_s + t_N}{\mathrm{min}} - 8 \cdot \frac{M_G}{\mathrm{m^3 t^{-1}}} - 4.3 \cdot \frac{M_L}{\mathrm{m^3 t^{-1}}} \quad (2)$$

where W_R is the specific electric energy demand, G_E is the weight of all ferrous materials, G_A is the furnace tap weight, G_Z is the weight of slag formers, T_A is the tapping temperature, t_s is the power-on time, t_N is the power-off time, M_G is the specific burner gas, and M_L is the specific lance oxygen.

By considering the parameters of the analyzed furnace and the lime reduction of 1000 kg of the injection procedures, the foreseen theoretical savings are equal to 20 kWh t^{-1}, which is in agreement with the electrical consumption obtained experimentally. In contrast, if the savings of the power-on time, methane, and oxygen consumptions brought by the injection procedures (discussed in the following sections) are also considered, the electrical savings value decreases to about 15 kWh t^{-1}. Therefore, it is possible to assume that the higher experimental values observed for both INJ1 and INJ2 procedures are due to the enhancing of the slag foamability, which is a parameter not considered in the model.

With an increasingly growing interest in reducing carbon dioxide emissions to fight against the greenhouse effect (not last The Paris Agreement[19]), the electrical savings were reflected in terms of equivalent tons of CO_2 not emitted. Assuming a typical scrap load of 88 tons and a total number of heat per year of 4950 (based on the 2016 Calvisano's production), 3460 t year^{-1} of not emitted CO_2 were estimated (equivalent factor = 0.2763 $kg_{CO2}kWh^{-1}$, according to ISPRA[20]). Moreover, a saving of 2341 TOE was calculated, which represent the amount of oil not burnt for the production of energy (**Table 2**).

3.3. Analysis of Methane Consumptions

Even for methane, the implementation of lime injection turns out in a significant reduction in consumption for both the class of steels, as shown in **Figure 6**. The change from lumps to injected lime led to a general reduction of ≈0.5 m^3 t^{-1} of the

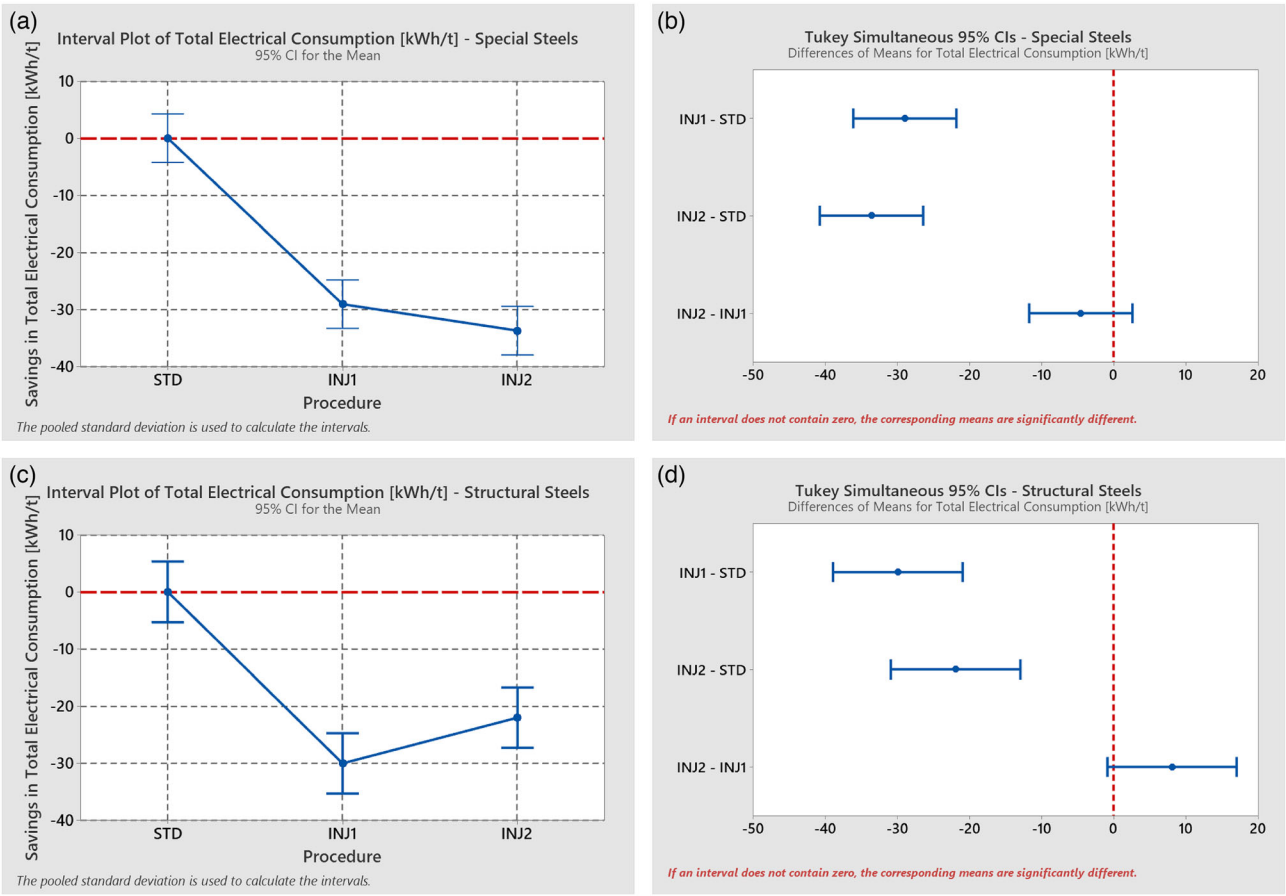

Figure 3. Variation of total electrical consumption switching from STD procedure to INJ1/2 procedures: a) interval plot, b) Tukey's comparison for special steels; c) interval plot, and d) Tukey's comparison for structural steels (values in kWh t^{-1}).

CH_4 consumption, with a slight increase in reduction when the INJ2 method was applied. The reductions can be related to the higher reaction rate achieved due to the injection of lime in fine particles, which guarantee an enhancement of the process efficiency. Moreover, it is possible to assume that the lower amount of slag produced, which will be analyzed later, less chemical energy was required for its heating; therefore, explaining the reduction of both the electrical and CH_4 consumptions for the structural steels production.

By converting the volume savings to electrical savings (by the use of high heat value conversion: 1 m^3 of methane develops 39.8 MJ m^{-3}[21]) and carrying out the same analysis made for the electrical consumption (average scraps loading of 88 tons and a total number of heats per year of 4950), the CO_2 emission was determined (equivalent factor = 0.2189 $kg_{CO_2}kWh^{-1}$, according to ISPRA[20]) as for the TOE (**Table 3**).

3.4. Analysis of Oxygen Consumptions

Figure 7 shows that the oxygen consumptions had a general decrease by switching from lump lime procedure to injected lime system; in particular, the difference between STD versus INJ1 and STD versus INJ2 was of ≈2.6 m^3t^{-1} and ≈1.6 m^3t^{-1}, for special steels (Figure 7a,b), and of ≈1.5 m^3t^{-1} for both STD versus INJ1 and STD versus INJ2, for structural steels (Figure 7c,b).

Referring to the case of special steel, the difference between INJ2 versus STD was expected to have a lower value. By considering the high quality of scraps, used for the production of special steels, it is possible to state that due to lower oxidation required for their production small fluctuation in oxygen consumption can be present. In addition, the small increment of oxygen observed between INJ1 and INJ2 compensates the reduction of energy consumption described before. Therefore, it is possible to correlate this weak increase in chemical energy provided by the oxidation reactions to the reduction of methane consumption, analyzed before, too.

3.5. Analysis of Carbon Consumptions

Figure 8 shows the analysis of the carbon consumptions added during the refining period for the slag foaming. As observable by the differences between the two procedures (Figure 8a–c) and the Tukey test results (Figure 8b–d), no statistically significant decreases were highlighted after the implementation of lime injection system for both special and structural steels.

In contrast, the great variability of the data emphasizes two aspect: the former highlights that the added carbon is used to

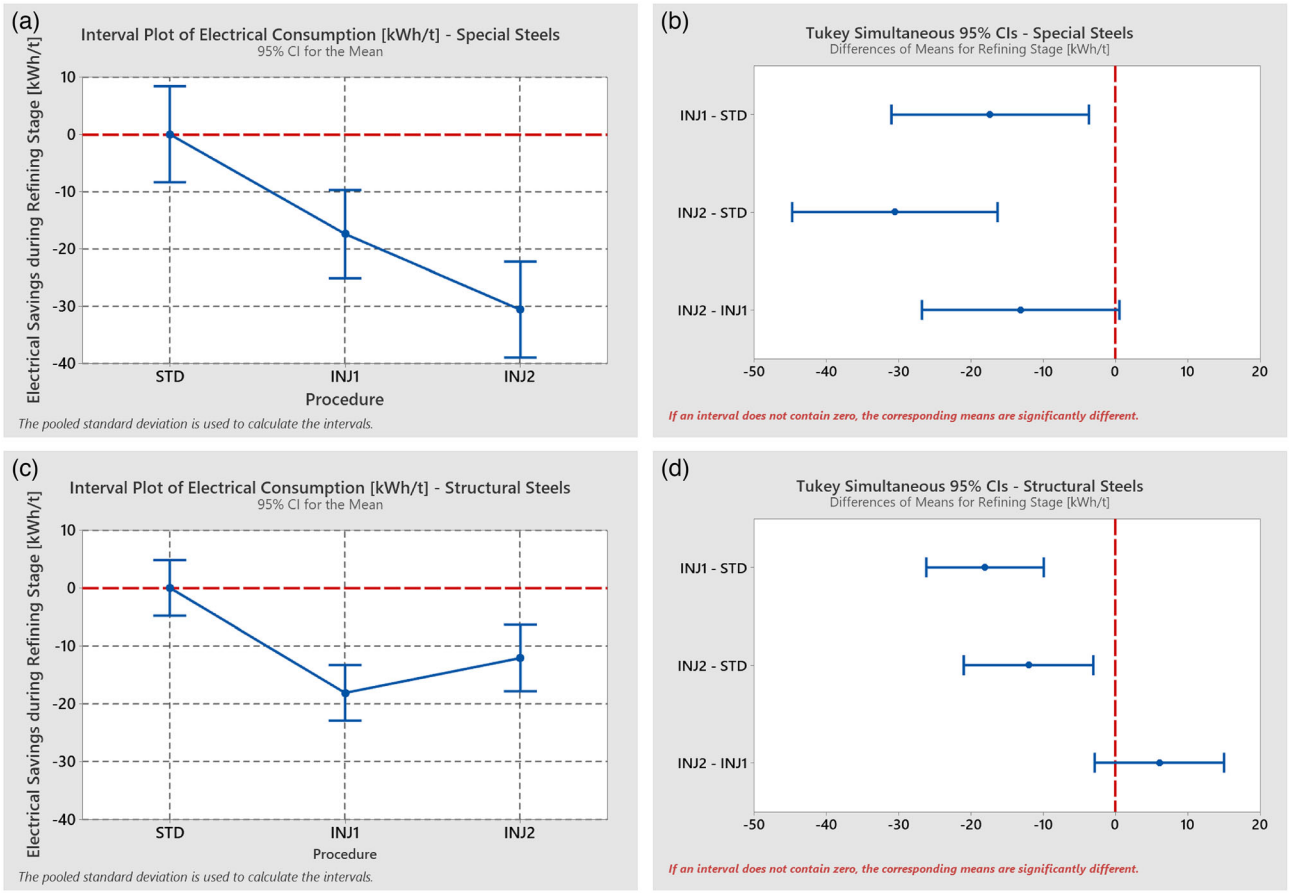

Figure 4. Variation of electrical consumption during the refining stage switching from STD procedure to INJ1/2 procedures: a) interval plot, b) Tukey's comparison for special steels; c) interval plot, and d) Tukey's comparison for structural steels (values in kWh t^{-1}).

control the carbon content in the bath, depending on the brand of steel to be produced; the latter is inherent to the fact that, probably, when the slag was foaming less, more carbon was injected, whereas if the slag had good foaming, it was used in lower quantity.

Briefly summarizing what has been analyzed by lime injection not only the consumption of electrical power was decreased but also oxygen and methane consumption decreased, in face of a stable amount of carbon injected (actually, slightly difference but not statistically significant was found). In particular, the switch from the traditional lime lump charging to the injected lime allowed a decrease in about 2800 TOE and 4500 $t_{CO_{2eq}}$, by only considering the reduction of electrical and methane consumptions. This better furnace behavior seems related to a better foaming of the slag, due to a better control of its quantity and quality. The next analysis will consist of verify and demonstrate that the identified improvement is actually attributable to better foaming control.

3.6. Analysis of the Foaming Capability of the Slag

To evaluate the slag foaming conditions, the ISD at 1600 °C has been recalculated with the method described by Pretorius.[13,14] The brands representing about the 80% of the production were compared. In particular, they are C82D2 and C82D2 + Cr for special steels, and S235JR and S275JR for structural steels. The slag range composition for such type of steels, for all the three procedures, is reported in **Table 4**. On the ISD diagrams (**Figure 9**), the blue dots represent every single heat belonging to the investigated brand (in term of slag chemical composition at the end of refining period), whereas the red dots represent the slag composition mean value of a certain numbers of heats.

Observing the scattered data points for special steels, shown in Figure 9a, it is possible to notice how, using lime in lumps (STD), they are moved up in respect of the optimum slag foaming condition. The mean value is significantly far from the upper liquidus line (or MgO saturation curve). This means that the slag is oversaturated in MgO and consequently too "crusty," and thus it tends to collapse even though an enough bubbles dispersion is formed within the slag. The excess of MgO in STD slag is due to an excess amount of CaO charged to obtain the proper P content, required by the specialty steels. This excess is also noted in the unusual value of the basicity index (BI_3). Usually, for steels of this type, it stands at values around 1.5–2, whereas in the current situation it reaches 2.5.[13] This excess lime was also charged to solve the difficulties of achieving a proper foaming slag, resulting in the opposite effect. Due to the impossibility to achieve an

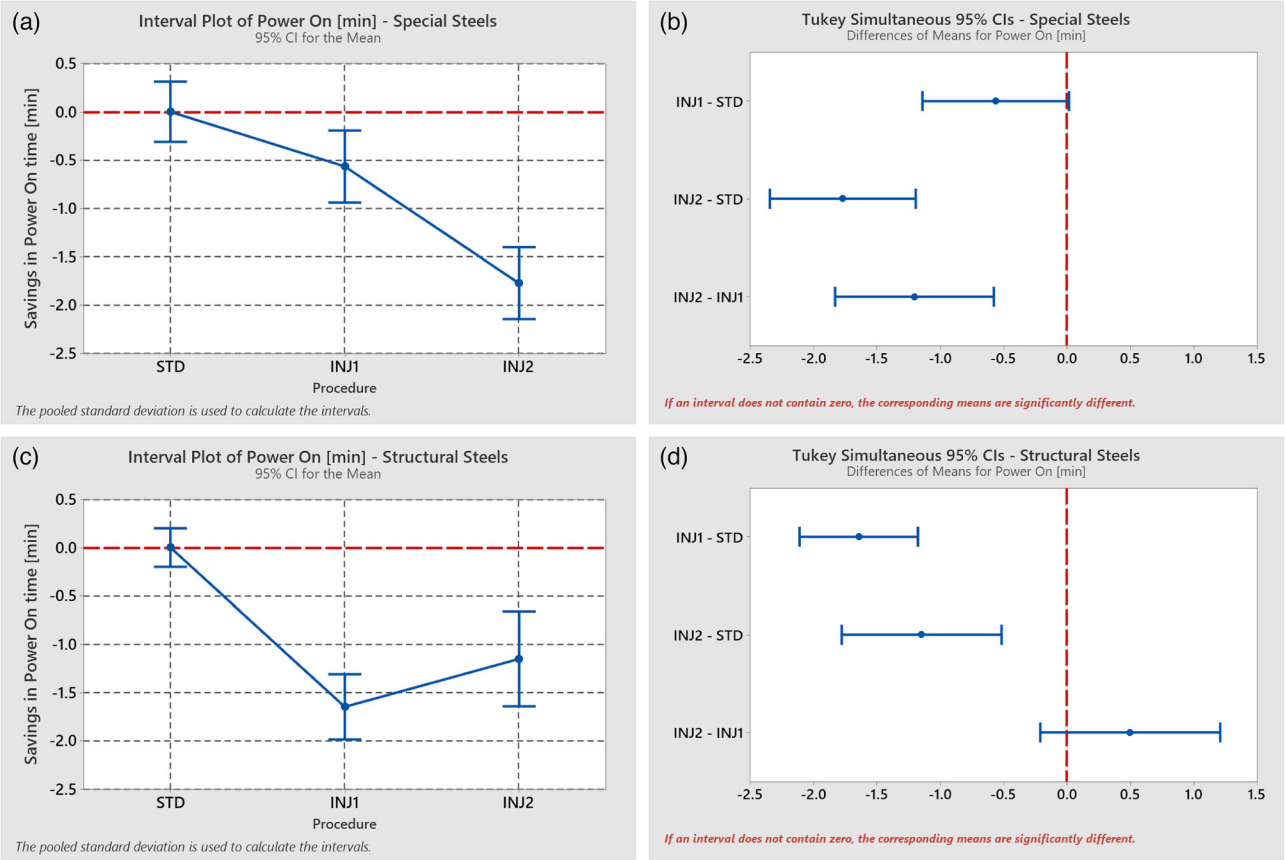

Figure 5. Variation of power-on time switching from STD procedure to INJ1/2 procedures: a) interval plot, b) Tukey's comparison for special steels; c) interval plot, and d) Tukey's comparison for structural steels (values in min).

Table 2. Summary of energy, TOE, and CO_{2eq} savings due to the lime injection adoption.

	Special-three buckets		Structural-four buckets		Mean
	INJ1	INJ2	INJ1	INJ2	
Specific savings [kWh t^{-1}]	30	35	30	20	
Annual savings [MWh $year^{-1}$]	13 068	15 246	13 068	8712	12 524
TOE saved					2342
Tons of not emitted CO_{2eq}					3460

optimum foamy slag, the arc could not be well covered, and this determine an appreciable refractories erosion on the EAF roof. Generally, using STD procedure, the roof refractories were changed every 2 weeks (data from steel shop internal evaluation). The assumption that a greater amount of slag to be heated, together with a worse foaming condition, has favored the increase in electrical consumption seems verified.

Injecting lime through INJ1 profile (Figure 9b) moves the representative points near the optimum foaming zone (except for few points under the MgO saturation) and the mean value is exactly on the MgO saturation. The slag seems to be correctly saturated with respect of MgO but is to be highlighted that points in the graph are representing the slag at the end of refining stage. Therefore, considering that the evolution of slag proceeds from a liquid phase to a more solid one, it is reasonable to assume that at the beginning of refining, the slag could be still liquid and thus not in optimum foamy condition. However, refractory lifetime increased by several weeks, confirming that a good foam, even during the last period of the refining stage, was reached. Using INJ2 procedure (Figure 9c), the slag composition slightly diverged from optimum condition, symptom that the largest amount of injected lime tends to oversaturate the slag, even the slag composition fits in the range where slag foaming is possible, and the arc covering can prevent energy losses in form of sidewall radiation. As for INJ1 procedure, in this case seems to be reasonable to presume that slag, at the start of refining, is just located near the ideal zone and during its evolution it moves to a more "crusty" zone. This means that during the slag evolution, it remains in an optimal foaming zone for longer time and this would explain the lower consumptions in INJ2, due to a better control of foaming. It is interesting to notice how the basicity (BI_3) is changed moving from 2.5 for STD to 1.75 for INJ1/2, which implies the shrinking of the liquid area as the slag basicity increases. This aspect, together with a more typical BI_3 index for the special steels production, makes it clear there is an excess of

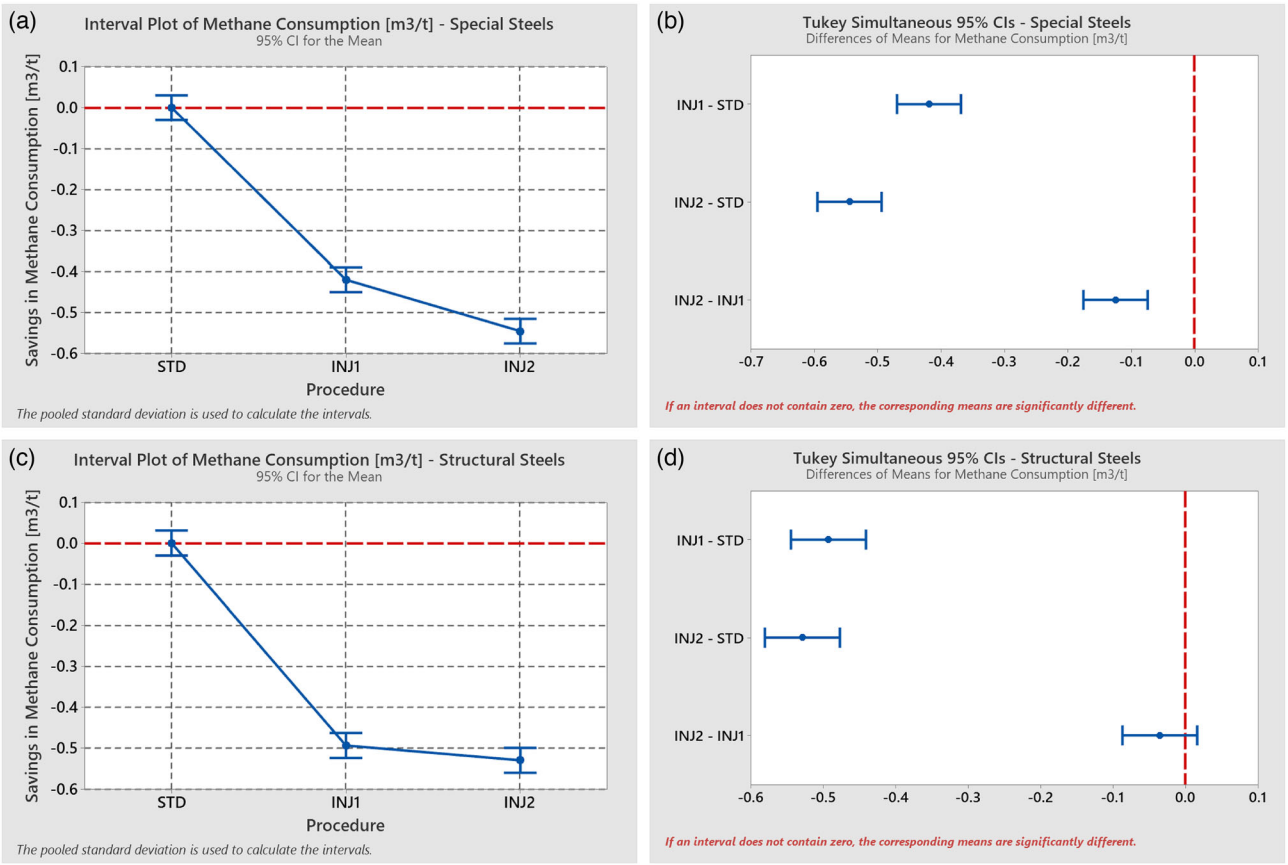

Figure 6. Variation of CH_4 consumption switching from STD procedure to INJ1/2 procedures: a) interval plot, b) Tukey's comparison for special steels; c) interval plot, and d) Tukey's comparison for structural steels (values in $m^3\,t^{-1}$).

Table 3. Summary of CH_4, TOE, and CO_{2eq} savings due to the lime injection adoption.

	Special-three buckets		Structural-four buckets		Mean
	INJ1	INJ2	INJ1	INJ2	
Specific savings [$m^3\,t^{-1}$]	0.4	0.55	0.5	0.55	
Specific savings [$kWh\,t^{-1}$]	4.3778	6.0195	5.4722	6.0195	
Annual savings [$MWh\,year^{-1}$]	1907	2622.1	2383.7	2622.1	2383.7
TOE saved					444.75
Tons of not emitted CO_{2eq}					521.79

lime in the STD procedure.[13] The scattering of the data suggests why the injected carbon values were scattered as well.

The same analysis was conducted for structural steels (Figure 9). With referring to STD practice (Figure 9d), the average chemical composition of the slag stands exactly on the liquidus line. This slag generally reaches the optimal foaming conditions, even at the end of refining stage. With the lime adjustment introduced by INJ1 procedure, differently on what was seen for special steels, the slag becomes undersaturated in MgO, thus, it seems to be much liquid. Because of the low viscosity of liquid phase, the residence time of the gas bubbles in the slag is shortened.[22] For this reason, the slag has difficulties to foam, and it deflates itself quickly (Figure 9e). This implies a limited arc covering, which generates a premature refractories erosion, shortening its lifetime. The slight increment of lime amount (≈200 kg) by INJ2 upgrade moves up the chemical composition of the slag close to the optimal foaming zone (Figure 9f). If on the one hand, switching from INJ1 to INJ2 profile improves the foaming conditions, on the other hand the same cannot be said for electric consumption, which are higher instead. This is probably because the addition of 200 kg more of lime maintains the same degree of bath oxidation (FeO %wt. is practically constant), is reflected on the need to heat up this additional amount by the arc. This also entails an extension of the power-on time.

The foaming conditions analyzed so far, are reflected in the THD value. Referring on the scale of values given before, the mean value of both special and structural steels for STD, INJ1 and INJ2 profiles are reported in **Figure 10**.

Observing the distortion values for the three procedures, it is possible to find consistency with the behavior noted through ISD. In particular, focusing on STD, THD results a value of ≈10.8 for special steels and 10.5 for structural steels. Although for structural steels, THD value is in agreement with

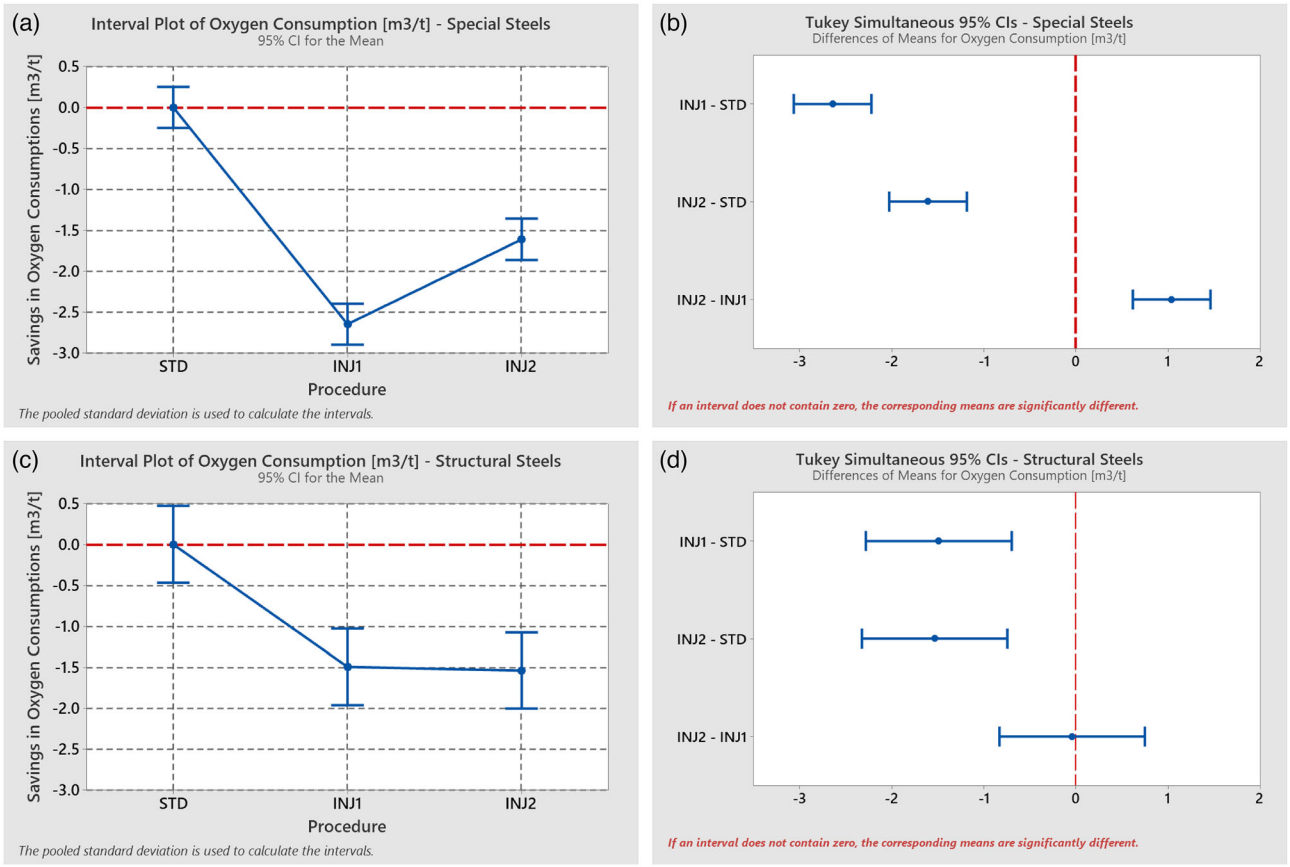

Figure 7. Variation of O_2 consumption switching from STD procedure to INJ1/2 procedures: a) interval plot, b) Tukey's comparison for special steels; c) interval plot, and d) Tukey's comparison for structural steels (values in $m^3\,t^{-1}$).

ISD analysis (Figure 9d), some differences can be highlighted for special steels (Figure 9a). For special steels, by use of standard lime addition profile, even the ISD suggests that the slag possess a high solid fraction at the end of refining stage, good foamability was still obtained. This was achieved by controlling the carbon powder injection to sustain the formation of a large volume of CO/CO_2 bubbles.[14,15]

Considering the INJ1 profile, a value of 10.5 for special steels attests that they reach the optimum foamability zone, as suggested in Figure 9b. The reduction in lime leads to a slightly reduction of injected carbon, still assuring an optimal arc covering. This is not true for structural steels: with a THD value of 11.5, the arc was not well covered, mainly caused by the large liquid fraction of the slag. Increasing the lime content with INJ2 procedure, the THD for special steels increases assuming a value of 11, reaching a condition similar to the STD procedure, where the slag chemical composition moved slightly away from the optimum foaming conditions. On the contrary, the structural steels show a distortion value of 10.5, which indicates they tend to foam better, approaching to the optimal condition, due to a reduction of liquid fraction and a good solid saturation of the slag (Figure 9f). Nevertheless, although a reduction of lime in slag, in both injection procedures, a good arc covering was achieved, as demonstrated by the reduction of refractory wear, from 2 weeks to 6 weeks of life.

Some slag samples were selected and the evolution of slag during the refining stage was analyzed, to understand if a correlation with distortion values is present. In **Figure 11**, the letters A and A′ represent the beginning and the ending of refining, respectively. Despite the examples shown by Pretorius,[14] where the slag proceeds from a "crusty" condition to a liquid one, all the sampled heats proceeded in the opposite direction. From a liquid zone, at the beginning of refining, to a more solid zone, at the end of refining.

In Figure 11a is reported the evolution of slag for a heat of a structural steel processed with STD procedure. From the start to the end of refining, the slag remains close to the optimum foaming and the derived distortion value varies between 10 and 11, confirming a good foaming behavior and a good arc shielding. According with Figure 11b, both at the beginning and in the end of refining, the slag is fully liquid and the THD value acquired was equal to 12. In this case, the heat was extremely poor in lime content as the basicity BI_3 was just 1. Fortunately, not all the heats performed with this procedure behave in this way. For some heats, a good foaming was achieved. In Figure 11c, a special steel produced using INJ2 profile is shown. The evolution proceeds from an optimum foaming zone to a more "crusty" zone and the distortion value acquired fluctuated around 11. However, this behavior highlights that with INJ2 pattern, the slag at the beginning of the refining process

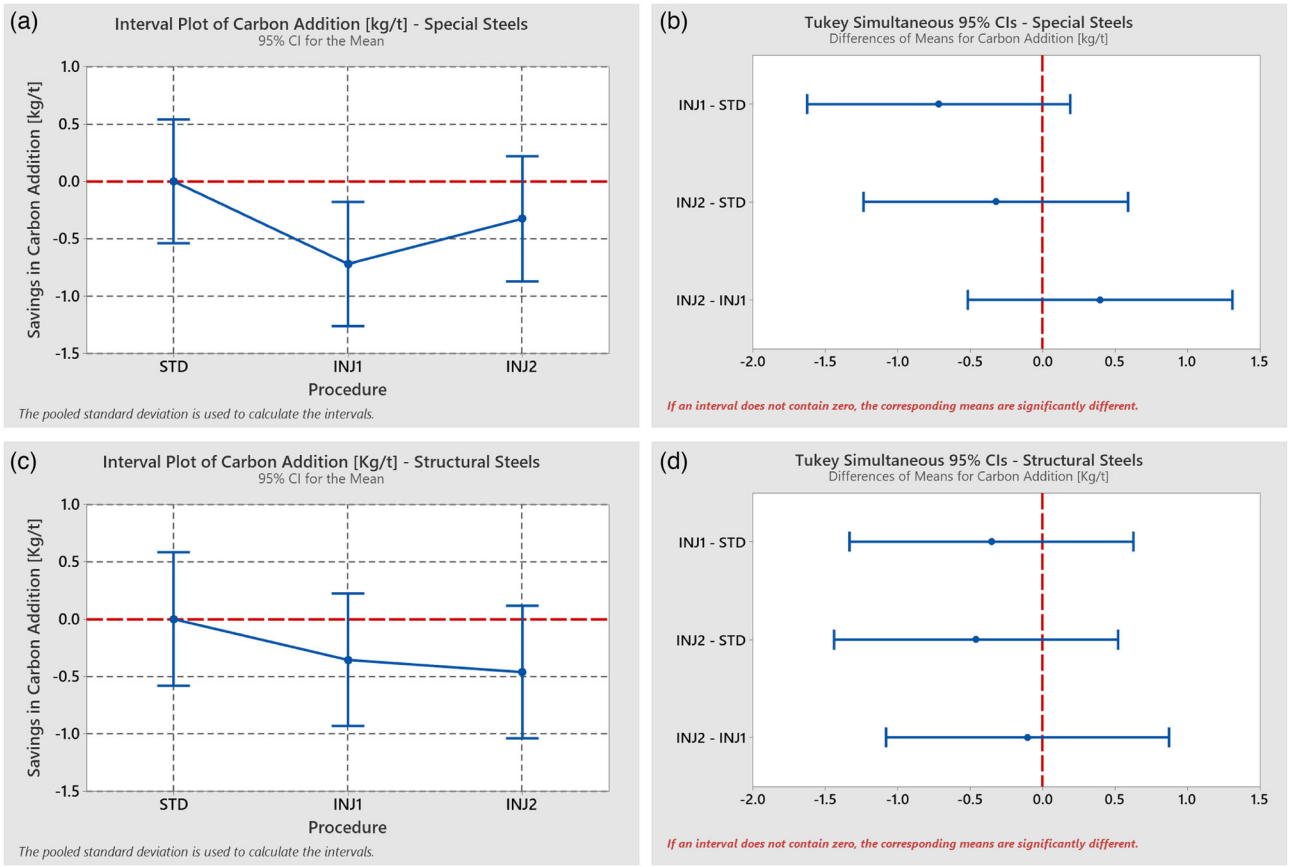

Figure 8. Variation of carbon addition during refining switching from STD procedure to INJ1/2 procedures: a) interval plot, b) Tukey's comparison for special steels; c) interval plot, and d) Tukey's comparison for structural steels (values in $kg\,t^{-1}$).

Table 4. XRF slag composition range (min–max) at the end of refining period (wt %).

	Special steels			Structural steels		
	STD	INJ1	INJ2	STD	INJ1	INJ2
Al_2O_3	3.07–7.42	3.07–7.12	2.84–5.31	3.84–10.43	5.33–8.15	5.97–7.15
CaO	23.02–42.75	22.49–39.57	22.55–37.04	21.26–37.13	22.01–26.29	21.89–24.54
Cr_2O_3	0.66–2.92	0.72–1.41	1.36–1.86	1.17–4.14	2.96–3.77	2.94–3.91
Fe_2O_3	12.21–44.37	15.54–40.73	26.37–50.43	23.16–42.99	35.15–45.05	36.99–45.21
K_2O	0–0.01	0–0.02	0.01–0.03	0.01–0.03	0.01–0.03	0.02–0.02
MgO	6.84–19.21	7–8.47	6.07–9.94	6.65–18.65	7.1–8.84	6.9–8.76
MnO	4.08–8.05	4.67–7.78	4.63–7.62	5.1–7.02	5.43–6.87	5.54–6.21
Na_2O	0.01–0.08	0.01–0.06	0.04–0.07	0.06–0.14	0.09–0.2	0.09–0.15
P_2O_5	0.25–0.73	0.41–0.66	0.38–0.55	0.3–0.58	0.41–0.64	0.4–0.57
S	0.02–0.09	0.04–0.11	0.03–0.06	0.04–0.08	0.04–0.06	0.04–0.06
SiO_2	6.22–14.74	9.49–16.01	9.06–13.63	8.58–14.09	8.69–12.86	9.9–11.7
TiO_2	0.3–0.74	0.28–0.63	0.22–0.47	0.35–0.49	0.36–0.47	0.35–0.43

possesses a good foamability which is then reduced progressively moving toward the end of the refining period. Nevertheless, starts the refining with good foam help to reduce the electrical consumption because the slag is yet ready to cover the arc. Starting the refining period with a fully liquid slag, even if it reaches the best foaming condition at the end of the refining period, is not an efficient process conduction, since for a certain extent of the heat, the arc is not shielded and the slag is not

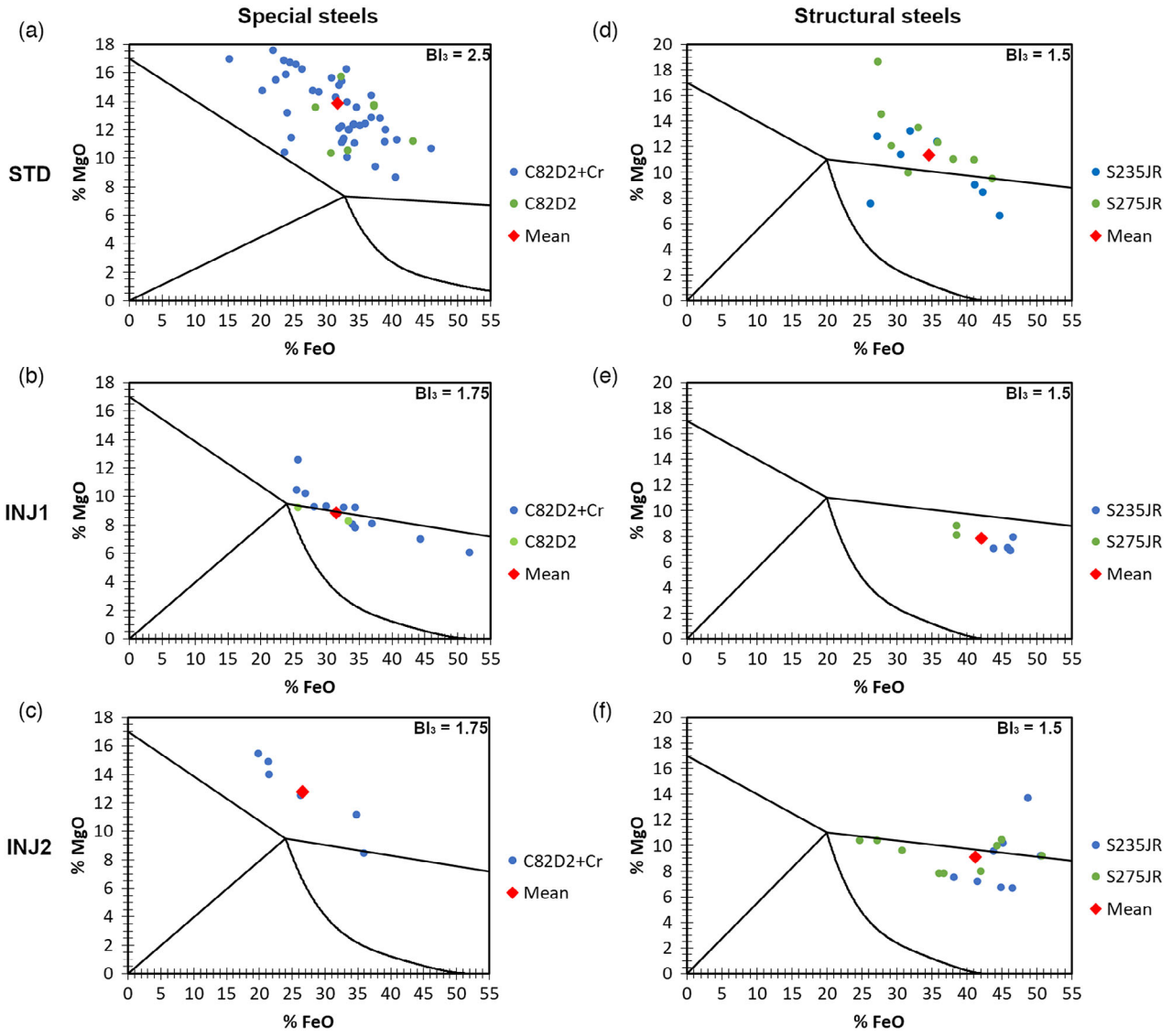

Figure 9. ISD at 1600 °C based on BI_3 for special steels: a) STD, b) INJ1, and c) INJ2 procedures and for structural steels d) STD, e) INJ1, and f) INJ2 procedures.

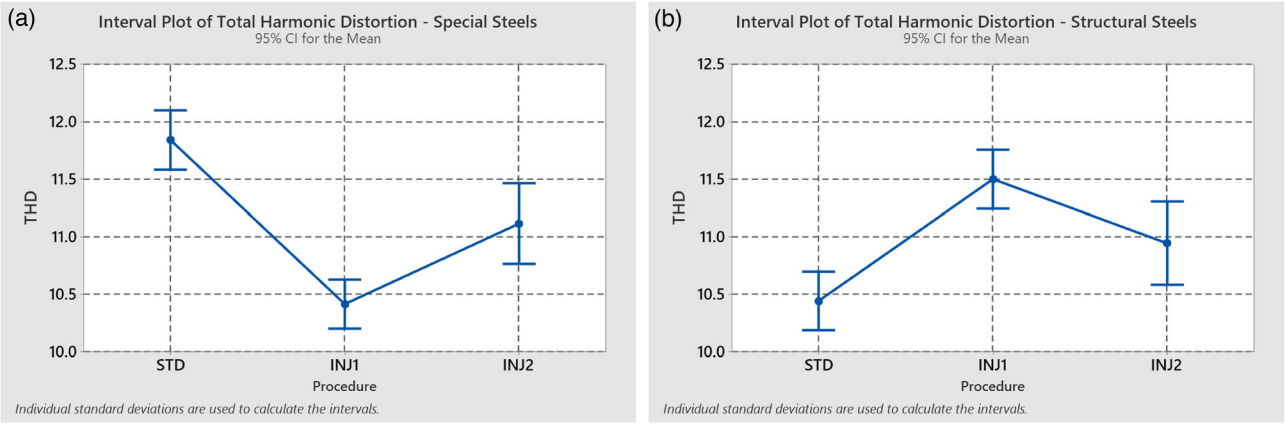

Figure 10. THD for: a) special steels; b) structural steels.

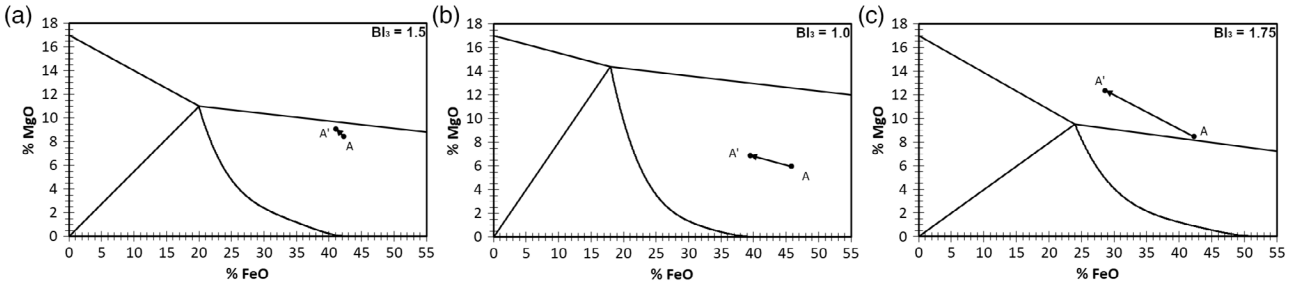

Figure 11. Examples of slag evolution from the beginning to the end of refining stage for a) STD procedure, b) INJ1 procedure, and c) INJ2 procedure.

saturated with respect to the refractories. This behavior can explain why for special steels, even the foamability seems slightly less using INJ2 procedure, the electrical energy consumption still decreases from INJ1 to INJ2.

3.7. Analysis of Slag Microstructure

The reduction in lime addition leads to a reduction of slag basicity (especially for special steels) that results in a different morphology and phases arrangement of the EAF slag. The typical phases identified for structural steels slag are wüstite ((Mn, Mg)O-FeO), brownmillerite ($4CaO{\cdot}Al_2O_3{\cdot}Fe_2O_3$), and dicalcium silicate ($2CaO{\cdot}SiO_2$). Exception might be chromium spinel ((Mg, Fe)$(Al,Fe,Cr)_2O_4$) or tricalcium silicate ($3CaO{\cdot}SiO_2$), the latter generally formed only if the basicity is high ($BI_3 > 2.5$).[23] Having a higher FeO content, they possess a pronounced dendritic structure as regards to wüstite. This is possible due to excess of liquid phase (FeO) in which nuclei are able to growth in the undercooled melt. According to this, moving from STD to INJ1/2, where a more liquid phase is present, the number of nuclei able to growth is higher and consequently the dendrites size decreases and presents a finer structure (**Figure 12**a,b). The dendrites average size fluctuates from 15 μm to 40 μm for the main arms and is 5–15 μm for secondary arms at the beginning of refining stage, whereas 5–10 μm for the main arm and 2–5 μm for the secondary arms at the end of refining. This happens because, at the end of the refining, a lower amount of FeO is present, which imply a less liquid phase, thus those few nuclei able to growth have no time to coalesce. As anticipated, having used a less amount of lime, the tricalcium silicate is not present using injection procedures, even if it appears sometimes in INJ2 samples. This is probably related to the extra quantity of lime used, which allow to generate tricalcium silicate in confined zones of the slag volume. Moreover, the lower BI_3 is, the finer dendrites are.

Special steels slag differs from the previous slag for the presence of tricalcium silicates due to the higher basicity. For instance, the 75% of samples have formed tricalcium silicate. Contrary to the structural steels, the special ones are less oxidized; for this reason, their structure is not strongly dendritic

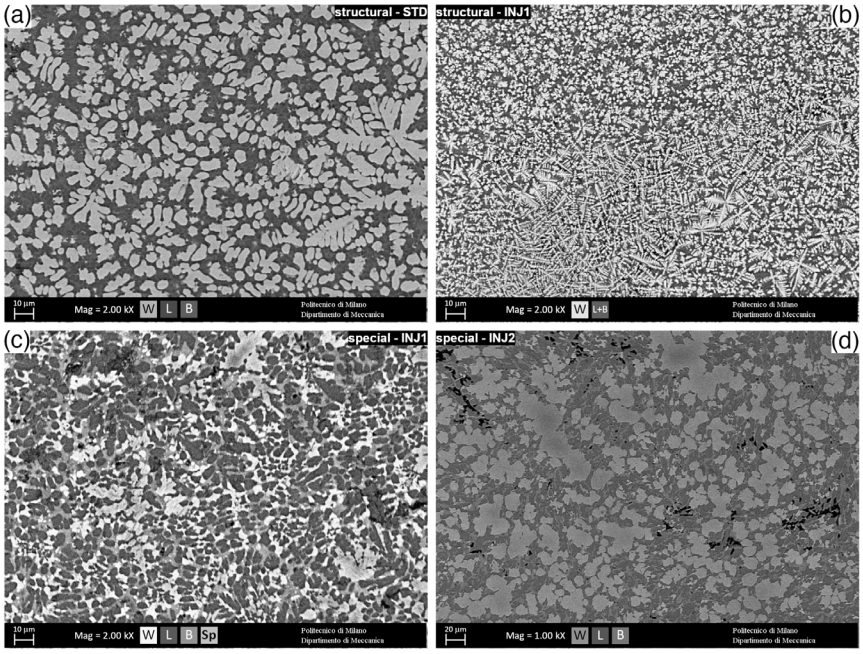

Figure 12. Examples of slag microstructure as a function of steel grade and lime addition procedure: a) structural steel STD, b) structural steel INJ 1, c) special steel INJ1, and d) special steel INJ2. B = brownmillerite; L = larnite; Sp = spinel; W = wustite.

(Figure 12c,d). It results in coarser wüstite crystals, with an average size from 2 μm to 20 μm, and with a coarser structure, where the more present compound is the ternary phase brownmillerite. The latter is finer for steels with injected lime and this is true for both the steel groups. In addition, the amount of CaO in brownmillerite is higher in the slag of special steels than those of structural ones. Special steels slag has high fraction of chromium: since these steels are designed for heat treatment, Cr is a fundamental alloying element to improve the quenchability.

The slag morphology looks slightly bigger in size moving to INJ2 procedure, but it does not seem to change with basicity, being the same for the analyzed samples, rather seems to be related to the additive quantity of lime which makes the slag less liquid, preventing the nuclei growth.

Tables with the range chemical composition, obtained through EDS analysis, of the earlier discussed phases per procedure are reported in **Table 5**.

3.8. Analysis of Slag Amount

To verify some of the hypothesis described earlier, the slag weight was measured and compared among the procedures.

For special steels (**Figure 13**a), the slag weight decreases switching from lime in lumps to injected lime. This can be related to the reduction of CaO consumption (Figure 2a), where the difference of ≈1000 kg between STD and INJ1 procedures is reflected in the slag amount reduction. The further decrease in slag amount, between INJ1 and INJ2, may be related to the fact that, for some specific special steel brands, the overall bath oxidation has been greatly reduced. This decrease appears to be counterintuitive with the increase in oxygen consumption reported in Figure 7a, by which an increase in slag amount should correspond. However, taking further into account the use of high-quality scraps, preferred for the production of special steels, the oxidation kinetic will be lower due to their high suface-on-volume (S/V) ratio.[17] Therefore, despite the additional 200 kg of lime used in INJ2 procedure, the final amount of slag is further decreased. The lower amount of slag has a positive impact on energetical consumption and the power-on time, which is confirmed by the trends previously observed from Figure 3a–6a.

For structural steels (Figure 13b) a similar trend is observed; the slag amount is reduced by switching from the traditional procedure to the injection ones, with a reduction of ≈900 kg for both INJ1 and INJ2 procedure. If compared to the special steels' slag amount reduction, the structural steels one is globally lower. However, a lower value of slag amount should be expected for the INJ1 procedure, in comparison to INJ2, due to the lower amount of CaO added (Figure 2c) and the constant value of oxygen used in the injection procedures of structural steels (Figure 7c). This behavior can be explained by considering the lower quality of scraps used in the production of structural steels. Usually, a large fraction of small old scrap is present, which, due to their high S/V ratio, increases the oxidation kinetics and the consequent slag amount.[17] Furthermore, always considering the scrap quality,

Table 5. Range chemical composition (min–max) of crystalline phases in the sampled slag by means of SEM–EDS..

Phase	Composition, wt.%						
	Mg	Al	Si	Ca	Cr	Mn	Fe
Structural steels—STD							
Wüstite	10.30–19.68	0.99–1.16	0.68	1.39–2.02	5.50–10.83	9.3–10.3	57.50–71.24
Brownmillerite	0.59–1.39	20.9–24.8		43.6–49.2	0.46	2.18–2.48	13.65–19.40
Dicalcium silicates	0.83–3.22	8.10–11.54	11.97–17.70	33.97–57.20	0.74–2.11	2.06–4.95	11.39–33.90
Tricalcium silicates	2.07	14.64	10.82	38.77	0.74	4.15	27.87
Chromium spinel	9.70	8.26	0.61	1.67	56.67	5.06	18.01
Structural steels—INJ1							
Wüstite	4.77–12.54	4.55–6.94	0.81–8.07	2.39–16.9	0.9–4.47	8.4–9.77	52.40–65.64
Brownmillerite	5.15	6.13	13.11	24	8.66	4.84	27.43
Dicalcium silicates	1.6–3.4	8.78–13.72	13.45–18.0	33.43–46.7	0.42–0.80	3.13–3.36	18.36–34.30
Chromium spinel	11.02	19.97		1.73	18.78	6.43	41.5
Special steels—INJ1							
Wüstite	5.89–37.30	<0.60	0.51–2.80	1.94–11.12	1.38–3.66	10.10–20.85	41.20–76.84
Brownmillerite	0.66–6.79	11.3–14.78	2.00–9.73	4.29–59.59	0.50–12.15	0.97–6.27	14.4–54.5
Dicalcium silicates		0.32–0.57	24–25	73.3		<0.60	1.36–1.52
Tricalcium silicates		3.39–3.93	13.90–17.93	58.0–73.3		1.16–3.31	13.39–21.90
Special steels—INJ2							
Wüstite	3.93–30.80	0.65–10.27	0.79–8.30	1.53–41.6	1.24–5.70	6.94–17.50	24.65–76.70
Brownmillerite	0.85–1.99	3.92–17.13	1.24–9.73	46.30–49.94	0.56–3.30	1.34–3.92	19.85–35.40
Dicalcium silicates	0.60–0.92	0.55–9.36	16.49–25.00	64.00–73.28		0.82–2.72	1.91–8.42
Tricalcium silicates	0.92–1.87	0.66–1.04	12.70–17.76	63.24–77.20		2.55–3.42	1.99–14.42

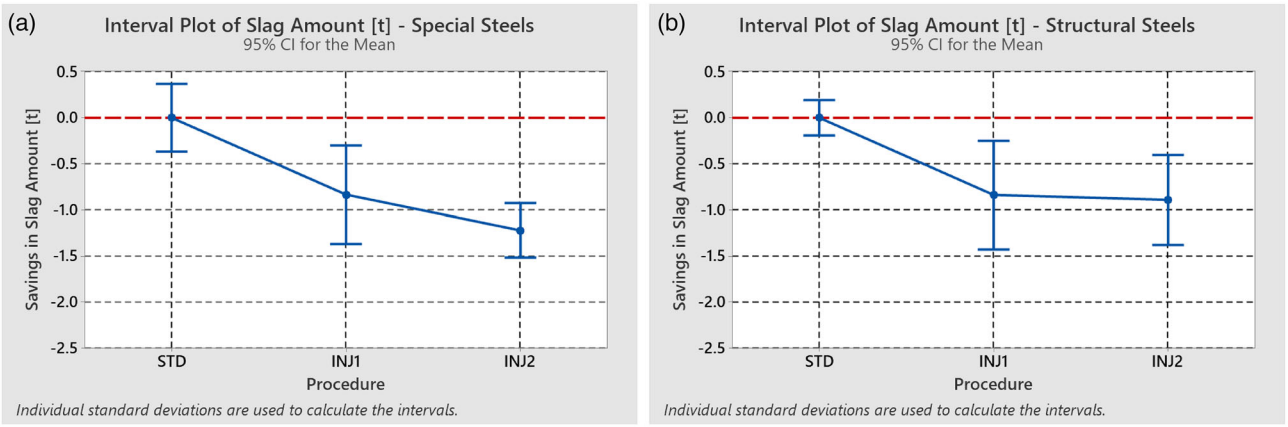

Figure 13. Slag amount variation switching from STD procedure to INJ1/2 procedures: a) special steels; b) structural steels (values in t).

a higher content of phosphorus should be expected in the bath. Therefore, a higher basicity of the slag is necessary to carry out an optimal dephosphorization, which explains the higher slag amount of structural steels in comparison to special ones. However, the switching from lime in lumps to injected lime did not alter the final P content of the steel (0.0025 ± 0.0021 wt% for structural and 0.017 ± 0.002 wt% for special steel), demonstrating that the optimization of lime addition is able to keep the same steel quality. The lower amount of slag has a positive impact on energetical consumption and the power-on time, which is confirmed by the trends previously observed from Figure 3c to Figure 6c.

Trying to relate both the slag amount and CaO addition reductions with the oxygen consumption, contour plots were prepared (**Figure 14**a,b). As for all the previous comparisons, the reference values used are the ones of the STD procedure heats.

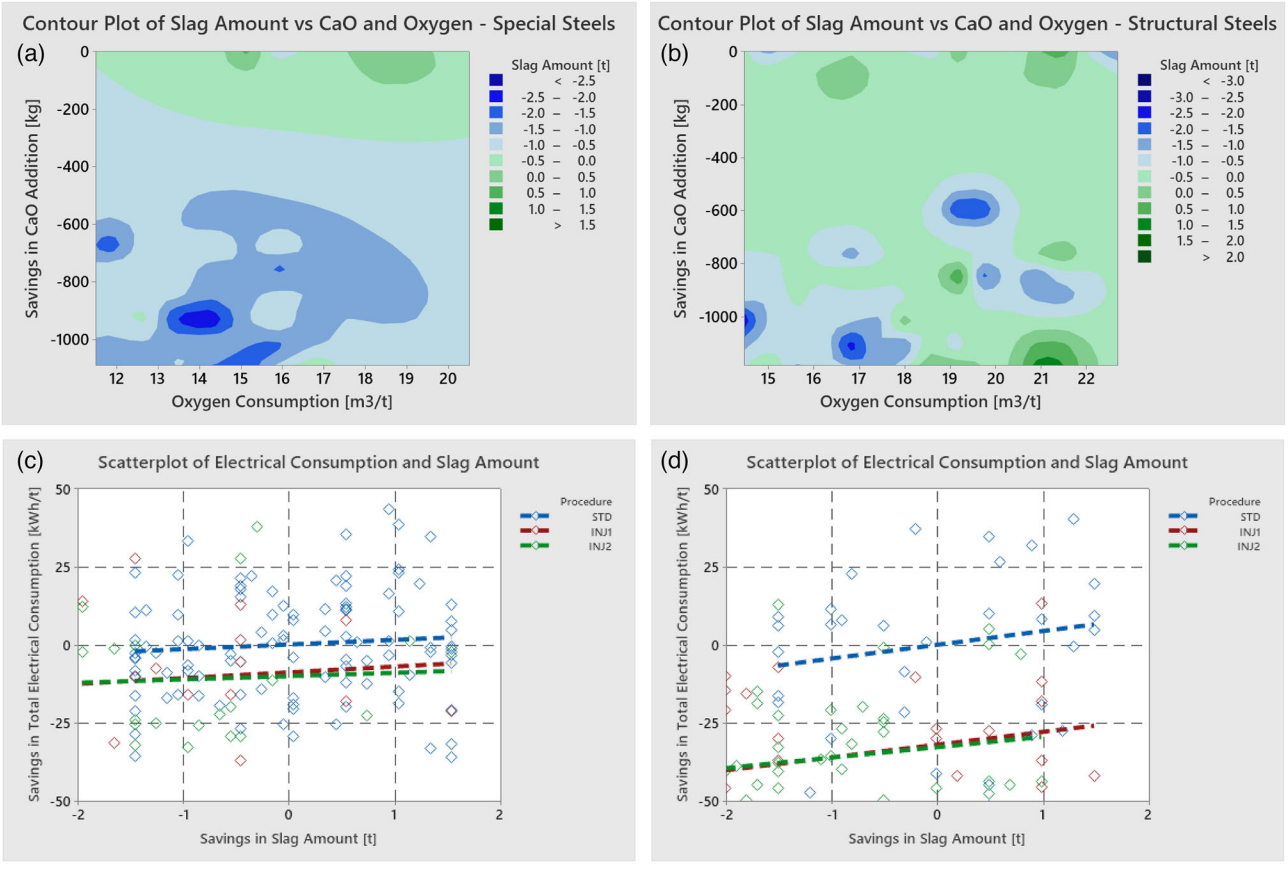

Figure 14. Contour plot of slag amount savings for a) special steels and b) structural steels (in function of lime savings and oxygen consumption) and slag amount-electrical consumption savings relation for c) special steels and d) structural steels.

The reduction of CaO has a significant impact on the special steels' slag amount, with a high reduction as soon as the lime is reduced. On the contrary, the oxygen consumption seems to be less effective and with an expectable trend: the lower the volume of oxygen used the lower the oxidation, with the maximum slag amount reduction obtained for 14 $m^3 t^{-1}$ of oxygen used. An opposite situation is observed in structural steels; the slag amount reduction is significant only after ≈500 kg lime saving and only with specific volumes of oxygen used. Such variability can be once again explained by considering the different quality of scraps used for the production of special and structural steels and the bath chemistry. Moreover, due to the four buckets charging procedure, used for the structural steels, the slag amount reduction is expected to be less significant and a higher amount of energy should be required for the heating of the bath, if compared with the three buckets procedure of special steels. This is confirmed by the relationship between the slag amount and the electrical consumption savings reported in Figure 14c,b. The lower amount of slag obtained due to the lime injection procedures allowed a reduction of the electrical consumptions of about one and a half times higher than the one observed for structural steels. No relevant differences were observed between INJ1 and INJ2 procedures.

3.9. Analysis of Metallic yield

An analysis on the iron contained in the slag under form of oxide has been conducted. It was defined a parameter called metallic yield as the ratio between the ferrous oxide mass (in the slag) and the mass of the liquid iron (in the EAF). This parameter can also be seen as a partition index of the iron contained in the slag and in the metal bath, the results are shown in **Figure 15**.

For what concern special steels, it is possible to observe that the differences between the standard and injection procedures are not significant, except for the difference between INJ1 and INJ2 procedure. In particular, the INJ1 procedure, having a lower amount of ferrous oxide in the slag, has a better performance in comparison with the INJ2 one. This is probably because that the oxygen consumption observed during the switch from the INJ1 procedure to the INJ2 one was higher (Figure 7a), whereas a limited decrease in the slag amount was observed (Figure 13a), thus resulting in a higher final amount of iron oxide in the slag.

For what concern the structural steels, it is possible to observe that the metallic yield values are higher in comparison with the one of special steels. This difference is probably due to the lower quality of scraps used for the production of structural steels and to a plausible higher fraction of high surface-to-volume ratio scraps used as charging materials, which led to a higher

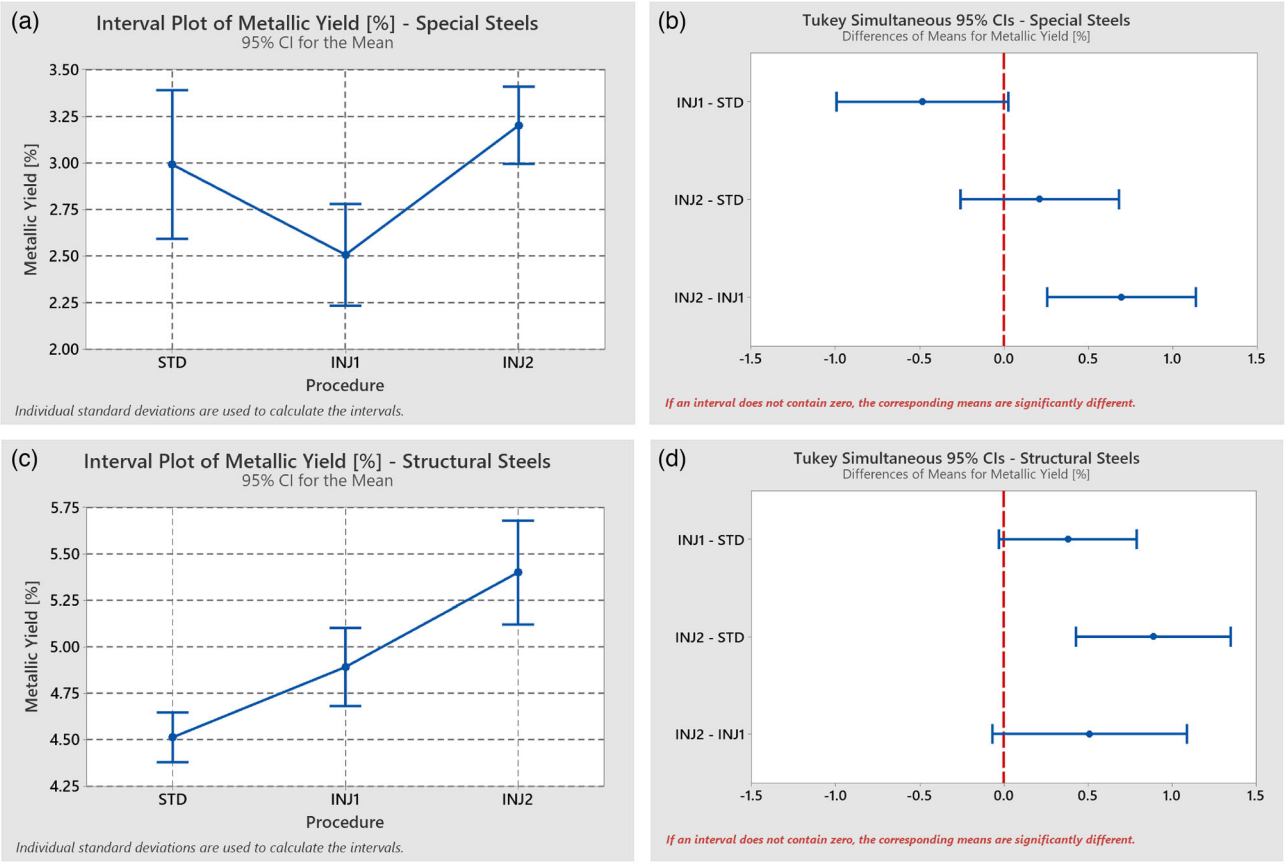

Figure 15. Variation of metallic yield switching from STD procedure to INJ1/2 procedures: a) interval plot, b) Tukey's comparison for special steels; c) interval plot, and d) Tukey's comparison for structural steels.

oxidation of the metal bath.[17] The only statistic significant difference, between the three procedures, is between the INJ2 procedure and the STD one. In particular, the former lead to a higher value of metallic yield. This increase can be caused by the limited changes observed in oxygen consumption (Figure 7c) and slag amount (Figure 13b) between the INJ1 and INJ2 procedures and to the higher amount of CaO of the latter procedure.

However, it should be considered that the increase in these values of metallic yield, meaning a higher amount of ferrous oxide in the slag with the same metallic bath mass, is very limited and such results should not affect the steel production process as much as the benefits previously discussed.

4. Conclusions

In this work, a new method to feed fine particles lime within the EAF of the Acciaierie di Calvisano steelmaking plant by the use of injectors was investigated. The aim of this work was to analyze and validate the benefits of lime injection compared to the traditional "lump charging" technique, which involves the use of lime in lump. To assess the potential advantages and the effectiveness of this new system, a comparison between the two practices have been performed. The study was done analyzing 1204 heats and sampling slag for 23 heats, both at the beginning and in the end of refining, for a total of 46 samples. In particular, the consumption of electricity, oxygen, methane, carbon, lime, and slag foaming capacity was investigated. The results of the new lime injection technique and the analysis made on the samples are summarized as follows: 1) the CaO consumption decreased considerably by ≈1000 kg switching from lump charging to lime injection; 2) the electric consumption was reduced by 20–30 kWh t^{-1}. Most of the saving (66.5%) is concentrated in the refining stage, whereas the remaining is due to a reduction of the power-on time of about 1–1.5 min as a function of the steel grade produced. All of this has meant an average 3460 t $year^{-1}$ of equivalent CO_2 and a TOE of 2342 savings; 3) the O_2 consumption was reduced by 2.5 and 1.5 m^3 t^{-1} using INJ1 and INJ2 for special steels and by 1.5 m^3 t^{-1} using both INJ1 and INJ2 for structural steels; 4) the CH_4 consumption was reduced by 0.5 m^3 t^{-1} for both special and structural steels, corresponding to a TOE of 446, allows a savings of 522 t $year^{-1}$ of equivalent CO_2; 5) the ISD investigation, then validated by THD analysis, has shown that the best foaming performances are reached using INJ1 for special steels and INJ2 for structural steels.

Considering the carbon tax, according to EPA (Environmental Protection Agency) who fixed the CO_2 social cost to 30 €/t (50 €/t not later than 2030[24]) the not emitted CO_2 corresponds to a saving of 117 180 €. Moreover, according to a study by the Stanford University,[25] the social cost saving associated to not emitted CO_2 can be equal to 722 608 €, for a CO_2 social cost estimated to 185 €/t.

Finally, it is advisable to use the INJ1 procedure for the special steels, whereas the INJ2 for the structural steels. For both the procedures, it is recommended to anticipate the time of lime injection, to start with a less liquid slag at the beginning to refining stage. For structural steels, it would be desirable to increase the quantity of injected lime, with respect to INJ2 procedure, by at least 200 kg, to reach a better foaming condition.

Conflict of Interest

The authors declare no conflict of interest.

Data Availability Statement

Research data are not shared.

Keywords

electric arc furnace, equivalent CO_2, isothermal stability diagrams, lime injection, tons of oil equivalent

Received: February 3, 2021
Revised: April 12, 2021
Published online: May 9, 2021

[1] Bureau of International Recycling – Ferrous Division, World Steel Recycling in Figures 2014–2018, Bruxelles, **2019**, https://www.bdsv.org/fileadmin/user_upload/World-Steel-Recycling-in-Figures-2014-2018.pdf (accessed: April 2021).
[2] World Steel Association, World Steel in Figures 2020, Bruxelles, **2020**. https://www.google.com/url?sa=t&rct=j&q=&esrc=s&source=web&cd=&ved=2ahUKEwim2KSS0sjuAhXV3oUKHSyvCbQQFjAAegQIBBAC&url=https%3A%2F%2Fwww.worldsteel.org%2Fen%2Fdam%2Fjcr%3Af7982217-cfde-4fdc-8ba0-795ed807f513%2F&usg=AOvVaw2uJu3DBo0zrMwgI8qMvLmK (accessed: April 2021).
[3] FederAcciai, La siderugia Italiana in cifre 2019, Milano, **2020**. http://federacciai.it/wp-content/uploads/2020/10/Assemblea2020_Siderurgia-in-cifre-2019_WEB.pdf (accessed: April 2021).
[4] L. Wolfe, *Overview of Lime Injection in the Electric Arc Furnace*, **2010**.
[5] L. Wolfe, J. Massin, T. Hunturk, W. Ripamonti, in *SCANMET III 3rd Int. Conf. Process Dev. Iron Steelmak*, Swerim AB, Luleå, **2008**: p. 10.
[6] H. S. Kim, D. J. Min, J. H. Park, *ISIJ Int.* **2001**, *41*, 317.
[7] T. X. Zhu, K. S. Coley, G. A. Irons, *Metall. Mater. Trans. B.* **2012**, *43*, 751.
[8] R. A. M. de Almeida, D. Vieira, W. V. Bielefeldt, A. C. F. Vilela, *Mater. Res.* **2017**, *20*, 474.
[9] A. A. Kozhukhov, V. V. Fedina, E. E. Merker, *Metallurgist.* **2012**, *56*, 169.
[10] A. Ghosh, A. Chatterjee, Ironmaking and Steelmaking Theory and Practice, **2008**. https://books.google.com/books?hl=en&lr=&id=7_GcmB4i_dsC&oi=fnd&pg=PA2&dq=+BOOK+Iron+making+and+steelmaking:+theory+and+practice&ots=vG47-o5X26&sig=I0EJjnIIaP1HRebThKvf8wGkWLM%0Ahttps://books.google.co.in/books/about/Ironmaking_and_Steelmaking.html?id=7_G (accessed: April 2021).
[11] W. Nicodemi, C. Mapelli, 1st ed., Associazione Italiana di Metallurgia (AIM), Siderurgia, Milano, Italy **2011**.
[12] D. C. Montgomery, *Design and Analysis of Experiments*, 8th ed., John Wiley & Sons Ltd, New York **2012**.
[13] E. Pretorius, *Fundamentals of Eaf and Ladle Slags*, **2004**, pp. 1–73.
[14] E. Pretorius, R. Carlisle, *Iron Steelmak.* **1999**, *26*, 79.
[15] D. Vieira, R.A.M. de Almeida, W.V. Bielefeldt, A.C.F. Vilela, *Mater. Res.* **2016**, *19*, 1127.
[16] D. Mombelli, C. Mapelli, S. Barella, A. Gruttadauria, R. Sosio, G. Valentino, V. Ancona, *Steel Res. Int.* **2018**, 89.
[17] D. Mombelli, G. Dall'Osto, C. Mapelli, A. Gruttadauria, S. Barella, *Steel Res. Int.* **2020**, https://doi.org/10.1002/srin.202000580.
[18] H. Pfeifer, M. Kirschen, J.P. Simoes, In *EEC 2005*, Birmingham, **2005**, p. 19.
[19] United Nations, *The Paris Agreement*, (**2021**). https://unfccc.int/process-and-meetings/the-paris-agreement/the-paris-agreement (accessed: February 2021).

[20] ISPRA, Rete Del Sist. Inf. Naz. Ambient, **2019**, http://www.sinanet.isprambiente.it/it/sia-ispra/serie-storiche-emissioni/fattori-di-emissione-per-la-produzione-ed-il-consumo-di-energia-elettrica-in-italia/view (accessed: April 2021).
[21] C. C. Clark, W. R. Hulsizer, in *Gas Turbine Mater. 1972 Conf.* (Ed.: C. L. Miler), Naval Ship Engineering Center, Hyattsville **1972**, pp. 35–42.
[22] S. Barella, A. Gruttadauria, C. Mapelli, D. Mombelli, *Ironmak. Steelmak.* **2012**, https://doi.org/10.1179/1743281212Y.0000000009.
[23] I. Z. Yildirim, M. Prezzi, In *IFCEE 2015*, American Society of Civil Engineers, Reston, VA, **2015**, pp. 2816–2825.
[24] QualEnergia.it, *Portare il prezzo della CO2 a 30 euro per tonnellata: la proposta francese*, **2016**. https://www.qualenergia.it/articoli/20160712-prezzo-della-co2-30-euro-tonnellata-la-proposta-francese-ETS/ (accessed: February 2021).
[25] F. C. Moore, D. B. Diaz, *Nat. Clim. Chang.* **2015**, *5*, 127.